The role of waves, shelf slope and sediment characteristics on the development of erosional chenier plains

Nardin William[1*] and Sergio Fagherazzi[2]

[1]Horn Point Laboratory, University of Maryland Center for Environmental Science, Cambridge MD USA 21613

[2]Department of Earth and Environment, Boston University, Boston MA USA 02215

*Author to whom correspondence should be addressed; E-Mail: wnardin@umces.edu;
Tel.: +1-410-221-8232.

Abstract

Cheniers are sandy ridges parallel to the coast separated by muddy deposits. Here we explore the development of erosional chenier plains, which form by winnowing during storms, through dimensional analysis and numerical results from the morphodynamic model Delft3D-SWAN. Our results show that wave energy and inner-shelf slope play an important role in the formation of erosional chenier plains. In our numerical experiments, waves affect the development of erosional chenier plains in three ways: by winnowing sand in the mudflats, by eroding mud at the shore, and by accumulating sand over the beach during extreme wave events. We further show that different sediment characteristics and wave climates lead to three alternative coastal landscapes: sandy strandplains, mudflats, or the more complex erosional chenier plains. Low inner-shelf slopes are the most favorable for mudflat and chenier plain formation, while high slopes decrease the likelihood of mudflat development and preservation, favoring the formation of strandplains. The presented study shows that erosional cheniers can form only when there is enough sediment availability to counteract wave action and for a specific range of shelf slopes.

1. Introduction

The word chenier derives from the Cajun name for oak, chêne, which is the prevalent tree encroaching sand ridges in southwestern Louisiana (Russell and Howe, 1935). In geomorphology, chenier is defined as a fossil sandy ridge amassed on muddy sediment and separated from the shoreline by a mudflat, formed by the deposition of fine cohesive littoral sediments (Byrne et al., 1959). The nature of the coastal ridges consists in deposits of sandy sediment, gravel or shell resting stratigraphically on mud (Otvos and Price, 1979). The aim of this work is to quantify how different sediment characteristics and wave climates can drive the stratigraphic genesis of the following three coastal landscapes: sandy strandplains, mudflats, or the alternate combination of the previous two formations, i.e. erosional chenier plains.

Previous studies have investigated chenier plains formation, without quantifying the key processes responsible for their occurrence. Chenier plains can be found in river deltas (Saito et al., 2000), in estuaries and bays, both in mesotidal or macrotidal systems (Otvos and Price, 1979; Woodroffe et al., 1983; Anthony, 1989; Park et al., 1996; Borrego et al., 2000; Morales et al., 2014). Draut et al., (2005) indicate that cheniers in Louisiana might have formed during strong storms in the presence of fluid muds and energetic wave climate. A recent study from Anthony et al., (2014) investigates the formation of one of the largest chenier plains system on Earth along the Guiana's coast of South America. These cheniers develop as a result of migration of mud banks from the mouths of the Amazon and Orinoco river deltas (Anthony et al., 2010; 2014).

In wave-dominated deltas, large ridge features form by wave-winnowing and remobilization of sand or shell fragments during energetic storms. In these settings muddy cohesive sediments cyclically separate a sandy-ridge system from the ocean with a development of a mudflat in front of the ridge. As a result, alternate ridges and mudflats, called erosional chenier plains, give rise to bands along the shoreline, as found for instance in Louisiana (Draut et al., 2005) and in the Mekong delta (Tamura et al., 2012; Nardin et al., 2016).

In other deltaic conditions, spit ridges develop at the mouths of delta distributaries, sheltering erosional backwaters that are subsequently filled with mud. These depositional chenier plains are typical of the Danube (Bhattacharya and Giosan, 2003) and Rhone deltas (Kruit, 1955).

Cheniers can also form with mechanisms different from the erosional and depositional cases. For example, the Chenier plains studied by Anthony et al., (2010) near the mouth of the Amazon River form by spatial variations in wave energy induced by the alternations of mud banks migrating alongshore and separated by inter-bank areas.

In this work we only study the formation of erosional chenier plains, caused by the the remobilization during energetic storms of lag coarse sediments in muddy tidal flats.

Augustinus (1989) discussed the origin of erosional cheniers when muddy deposition at the shore is disturbed by a high energy events resulting in a sandy or shell deposit. However, this study did not quantify under what conditions this system form or modeled in detail the physical processes at play.

A different landform created by high energy waves is a strandplain, which is a broad accumulation of sand in parallel deposits or dunes along the shoreline (Hein et al., 2013; Otvos and Price, 1979). Contrary to cheniers, strandplains are not separated by mud deposits. Here we will determine under what conditions a strandplain or an erosional chenier plain form at the shore.

Roy et al., (1994) determined that strandplains are frequent along coasts with high waves, rich in sediments, and facing wide and gentling sloping continental shelves. Strandplains and chenier plains are common landscapes worldwide (Franceschini and Compton, 2006). They are present in Australia on the gulf of Carpentaria (Chappell and Grindrod, 1984; Woodroffe and Grime, 1999; Harvey, 2006; Nott et al., 2009), in Egypt on the Nile delta (Goodfriend and Stanley, 1999) in Brazil (Hein et al., 2013), and along the West coast of Africa (Anthony, 1995).

In our study, we carried out a set of numerical simulations with the numerical models Delft3D (Lesser et al., 2004) and SWAN (Booij et al., 1999) to generate a database for a theoretical investigation on the formation of erosional chenier plains using dimensional analysis. The stratigraphic module of Delft3D is used to generate and record deposition of alternate sediment layers. The same numerical framework was recently used to explore the impact of waves on coastal morphology (Nardin & Fagherazzi, 2012; Nardin et al., 2013) and the effect of tides on the alternate deposition of mud and sand (Leonardi et al., 2014).

2. Dimensional Analysis

Most published work focuses on chenier morphological and sedimentological characteristics around the world (Russell and Howe, 1935; Byrne et al., 1959; Augustinus, 1989). These studies address the physical mechanisms responsible for chenier genesis from a qualitative point of view. Our goal is to build a process-based rationale centered on dimensional analysis of numerical results.

As usually present in many chenier plain locations, we study a schematic case of a seaward slope in front of an approximately plane mudflat (Figure 1). This conformation refers to the broadly observed study case in which sediment resuspension by waves is capable of displacing the sediment stored at the shoreline.

Erosional chenier plain genesis can be divided in two main stages: formation of a sandy ridge and formation of a mudflat in front of the ridge. The dynamics of ridge formation depend on wave energy during extreme storms and the nature of the non-cohesive sediments present on the shelf. The initial seaward slope plays a crucial role in sediment winnowing and in the morphological response to wave action.

We assume that significant wave height, H_S (associated with a critical shear stress, $\tau_{ws,}$ during storms event), and sediment characteristics (grain size, D_{50}, and density, ρ_s) are the driving variables for the development of the sandy (or shell gravel) ridge. The second stage of chenier formation is the deposition and subsequent progradation of a mudflat in front of the sandy ridge during fair-weather conditions. Mudflat formation mainly depends on the properties and availability of cohesive sediments, dictated by concentration, c_m and settling velocity, w_s. Because the mudflat is subject to wave attack, erosion from small, fair-weather waves is present during the mudflat formation cycle. We recognize the importance of other two variables: wave bottom shear stress during fair-weather conditions, τ_w, and critical shear stress for mud erosion, τ_{cr}, stating the predisposition of the bottom substrate to be resuspended by waves. The list of relevant processes is completed by including erosion during extreme storms that can considerably reduce the mudflat extension.

We have thus identified a list of variables indispensable to describe chenier formation during the two stages of sand ridge formation and mudflat progradation: 1) basinward slope S [L L^{-1}]; (2) sediment density ρ_s [M L^{-3}]; (3) mean diameter of sand or shell gravel D_{50} [L]; (4) average cohesive sediment concentration in the water column c_m [M L^{-3}]; (5) critical shear stress for erosion τ_{cr} [M L^{-1} T^{-2}]; (6) settling velocity of mud w_s [L T^{-1}]; (7) wave bottom shear stress τ_w (and τ_{ws} in case of extreme storms) [M L^{-1} T^{-2}]; (8) erodability of mud deposits M_e [M L^{-2} T^{-1}]; where length, L, time, T, and mass, M, are the fundamental units of the problem. We apply the Buckingham's theorem of dimensional analysis (Langhaar, 1951) stating that the explanation of chenier genesis can be expressed in terms of 5 non-dimensional parameters, which can be chosen among all potential couples of independent non-dimensional groupings. We select the inner-shelf slope and a combination of the following 4 non-dimensional groups:

$$\Pi_1 = S\,;\ \Pi_2 = \frac{\tau_{ws}}{(\rho_s - \rho_w) g D_{50}};\ \Pi_3 = \frac{\tau_w}{\tau_{cr}};\ \Pi_4 = \frac{c_m w_s}{M_e}\ ;\ \Pi_5 = \frac{\Pi_4}{\Pi_3} \qquad \text{(1a,b,c,d,e)}$$

where Π_2 is the susceptibility of sandy sediments to resuspension during storms, Π_3 is the susceptibility of mud deposits to erosion during fair-weather events, Π_4 is the ratio between fine-sediments potential deposition and potential erosion.

The formation of sandy ridges is then defined by a relationship between the two non-dimensional variables Π_1 and Π_2.

$$\frac{\tau_{ws}}{(\rho_s - \rho_w) g D_{50}} = f(S) \tag{2}$$

mudflat formation is described by Π_1 and Π_5:

$$\frac{c_m W_s}{M_e \frac{\tau_w}{\tau_{cr}}} = g(S) \tag{3}$$

while mudflat erosion during storms is dictated by Π_1 and Π_3:

$$\frac{\tau_w}{\tau_{cr}} = h(S) \tag{4}$$

where $f(S), g(S),$ and $h(S)$ are unknown functional relationships to be determined through numerical experiments. It is important to note that equations (2), (3), and (4) were directly derived from the definition of the principal variables and from the theorem of Buckingham.

3. Numerical model

3.1 Model description

Chenier plains evolution is investigated coupling the computational fluid dynamics model Delft3D with the wave simulator SWAN. Delft3D resolves the bi-dimensional shallow-water equations, using the computed velocity field to determine geomorphological evolution. The generation and propagation of waves in shallow water is computed by SWAN. Delft3D solves the continuity equation and the horizontal momentum equations, using a turbulence closure method. Vertical accelerations are not taken into account, because they are supposed to be small compared to the gravitational acceleration. The vertical momentum equation is therefore approximated to the hydrostatic pressure relation (Lesser et al., 2004).

Bedload and suspended transport of cohesive and non-cohesive sediments are modeled by the sediment transport and morphology modules. The Van Rijn (1993) formulation is used to calculate bedload transport. Suspended-load transport is modeled with the 3-dimensional diffusion-advection formulation with the sediment eddy diffusivity and viscosity set at the same value. The vertical eddy viscosity applies the standard k-ε closure formulation (Rodi, 1984) for all runs. A large eddy simulation technique is used to account for the horizontal eddy viscosity. SWAN can mimic random, short-crested waves in the open ocean and in shallow water regions. The key processes incorporated in SWAN are: wave-wave interactions, wave refraction, and wave dissipation. The dissipation term includes bottom friction (Hasselmann et al., 1973), whitecapping (Komen et al., 1984), and wave breaking (Battjes and Janssen, 1978).

Our runs are planned to explore the hydrodynamic and morphological settings of waves with different energy levels propagating into a coastal region with variable slope. We also explore the presence of sediments with different characteristics. Because chenier plain genesis is complex, we have limited our investigation to two different wave energy levels and two sediment types. In the first stage, ridge formation, high energy waves attack the mudflat, which has a small fraction of sandy sediments. Storm waves of short duration partially erode the mudflat. At the same time, waves and related wave setup wash over the sandy sediments accumulating them at the shore and thus forming a sandy ridge. In the second stage of chenier formation, mudflat extension, a low and constant wave energy coupled with high concentrations of cohesive sediments is assumed, such that waves can carry and deposit the sediments on the mudflat without eroding the substrate.

3.2 Numerical model set-up and simulations

We present modeling results on how waves and sediment characteristics can drive the process of chenier plain formation in a rectangular basin with rectangular cells, whose long cell dimension is along the coast (Fig. 1a). The grid has 50 by 50 computational cells, each of size of 100x20 m and it is finer along the cross-shore direction to better model wave propagation. Model runs are divided in two parts: chenier formation and mudflat establishment. Both use the same domain but with different sediments, waves, and basin slopes.

We start from a mudflat with a 10% sand content and a constant slope. We then apply a storm event, which erodes part of the mudflat and generates an accumulation of sandy sediments at the shore. Afterward, fair-weather conditions are simulated resulting in the formation of a new mudflat in front of the ridge. The run is then stopped and restarted with the same bed level configuration but replenishing the initial content of sand in the sediment deposited in the mudflat (10%). This allows to always have available sand in the shelf sediments to build a new chenier. A new storm event is then generated. After several runs a new chenier forms. We simulate two-day storm every ten years, then ten years for mudflat progradation with fair-weather waves.

The basin has an initial slope between 0.004 and 0.013 along the east-west direction, creating an initial water depth at the West boundary between 6 and 20 m. The initial bed level is planned to represent an initial mudflat configuration. A white-noise perturbation between 0 and 5 cm is superimposed to the bottom elevation to simulate the natural variability of the shelf substrate. Sensitivity tests show that the shoreline extension in both directions of the computational domain does not change the results of the study. The North, South, and East boundary conditions are zero elevation water level (Figure 1). A five meters deep layer of mixed cohesive and non-cohesive sediments is originally accessible for erosion at the bottom of the domain.

We first carry out 164 simulations with negligible equilibrium concentrations of non-cohesive sediments at all boundaries. We use three diameters, D_{50}, for the sand fraction (100, 200 and 1,000 μm). The specific density of the sediment is 2,650 kg m^{-3}, while the dry density of the bed is 1,600 kgm^{-3}. Characteristics of the cohesive sediment are chosen in agreement with values provided by

Berlamont (1993). Specific density is 2,650 kgm^{-3}, dry bed density is 500 kgm^{-3}, settling velocity varies from 0.05 mm s^{-1} to 0.5 mm s^{-1}, and cohesive sediment concentrations of 0.4 and 1.0 kg m^{-3}.

In case of cohesive sediments, the Partheniades–Krone formulation for erosion and deposition are used (Partheniades, 1965). In this formulation, the critical shear stress for erosion is always greater than or equal to that for deposition. The horizontal eddy-viscosity coefficient is defined as the combination of the subgrid-scale horizontal eddy-viscosity, computed from a horizontal large-eddy simulation, and the background horizontal viscosity here set equal to 0.001 m^2 s^{-1}. We used a morphological factor of 500 to speed-up our model runs, after we define that the final result was not influenced.

Wave parameters (H_s and T_p) are selected to simulate waves generated in the ocean. We vary H_s between 0.1m and 3m, and use a period, T_p of 5s during mild-weather conditions and 10s during storms. In order to investigates the sandy ridge formation with the higher slope of S=0.013, we model highly energetic waves with H_s = 4m. We impose wave period and significant wave height at the East boundary, orthogonal to the shoreline avoiding any major alongshore current development. Wave reflection is not accounted for in the wave model so that wave energy is dissipated at the coastline.

4. Results and discussion

As a first result, we plot $\frac{\tau_{ws}}{(\rho_s-\rho_w)gD_{50}}$ versus S in Fig. 2a, which, based on equation (2), offers a characterization of $f(S)$. We find that the formation of a sandy ridge for different wave heights and grain sizes depends on bottom slope. For high slopes (larger than 0.015) it is always hard for waves to build a sand ridge. Therefore, a threshold in S exists above which ridge formation is prevented.

We then study the impact of the percentage of sand in bottom sediments on ridge formation. Results with a sand percent of 10% and 25% do not differ. We therefore plot only the results with 10% of sand in our figures. During storms, waves can remove and re-suspend the entire fine sediment fraction at the shelf bottom while the non-cohesive sediment is accumulated at the beach forming a sandy ridge.

To better understand the dynamics of ridge formation displayed in Figure 2a, we analyze in detail the equations governing sediment transport of sand by waves. In SWAN (Booij et al., 1999) the waves induced shear stress, τ_w (τ_{ws} in case of storms) is calculated as:

$$\tau_w = \frac{1}{2}\rho f_w u_b^2, \qquad u_b = \frac{\pi H_s}{T_p \sinh(KD)} \qquad (5a,b)$$

where ρ is the fluid density, u_b is the wave bottom orbital velocity, H_s is the significant wave height, T_p is the wave peak period, D is the domain depth, K is the wave number, and f_w is a wave friction factor, calculated as:

$$f_w = \begin{cases} 0.00251\exp\left[5.21\left(\frac{u_b}{\omega k_s}\right)^{-0.19}\right] & ; \frac{u_b}{\omega k_s} > \frac{\pi}{2} \\ 0.3 & ; \frac{u_b}{\omega k_s} < \frac{\pi}{2} \end{cases} \qquad (6)$$

where ω is the angular frequency, k_s is the Nikuradse roughness, estimated as 3.5 times the median sediment grain size, D_{50}. A more detailed discussion of the SWAN model can be found in the supporting information (Grant and Madsen, 1979; Soulsby et al., 1993a).

From these equations an increase in median grain size of sand, D_{50}, leads to an increase in roughness, k_s, and consequently friction, f_w, while the bottom shear stress, τ_w, decreases. As a result, there is less erosion for large grain sizes. Moreover, from the Shields parameter a higher grain size requires a higher bottom shear stress in order to mobilize the sediment. An increment in significant wave height enhances the bottom orbital velocity, and therefore bottom shear stress, τ_w. Consequently, higher waves erode more sediment. The non-dimensional number $\frac{\tau_{ws}}{(\rho_s-\rho_w)gD_{50}}$ therefore represents the potential mobilization of bottom sediments (Shields parameter for waves).

Bottom erodibility also depends on inner-shelf slope, and an increasing in nearshore slope leads to a narrow surf zone close to the beach. High slopes thus imply a reduced potential for sand entrainment on the shelf (Figure 2a). This is the reason why for steep shelf slopes it is hard to erode sand from the bottom and generate a sandy ridge. This is in accordance with Hein et al. (2013), who show that a low shelf slope and high energy waves favor the formation of strandplain in Pinheira, southeastern Brazil. The ratio between wave bottom shear stress, τ_w, and critical shear stress for mud erosion,τ_{cr}, represents the potential wave erosion of the mudflat. τ_w is computed at the east boundary and strongly depends on H_s. Our simulations show that the mudflat is preserved in the presence of weak waves or very consolidated mud. By increasing the bottom slope, we decrease mudflat preservation, since energetic waves break near the shore eroding the mud (Fig. 2a). On the contrary, a mild inner-shelf slope favors wave energy dissipation across a wide area of the shelf, so that the incoming waves never have enough energy to resuspend the muddy sediments.

Figure 2b displays the relationship between the non-dimensional variables controlling mudflat formation and shelf slope. Our results show that for gentle slopes a high range of Π_5 values lead to mudflat formation while in steep inner-shelves it is difficult to deposit cohesive sediments. This is due to a balance between deposition (at the numerator of the non-dimensional number Π_5) and erosion by waves (at the denominator). In fact, waves have a twofold effect, they move sediment to the shore through wave-breaking and wave drift but they can also erode sediments from the bottom. Only when the first process dominates you have mudflat formation.

In our runs, we want to grow a mudflat from the shore. Intermediate and high values of sediment concentration can generate the initiation of a prograding mudflat. Low values of sediment concentrations are not sufficient to overcome the mild wave erosion caused by fair-weather waves (Figure 2b).

Potential mudflat erosion during storms is an additional important process during chenier plains evolution. In our model simulations, if complete mudflat erosion occurs during a storm then a new sand ridge is deposited in contact with the old ridge without mud deposits in between. In this case, we classify the system as a strandplain, since the model would continue to deposit sandy ridges side by side leading to long-term progradation.

To better understand erosion by waves on a mudflat we analyze shelf elevations and maximum bed shear stress after storms for four numerical test cases (Figure 3). For a fixed wave peak period of 10s, mudflat erosion increases for higher wave heights and for lower shelf slopes (Figure 3a). Maximum bed shear stress with 3 m waves is four times higher than with waves of 1 m (Figure 3b) and maximum values are observed where waves break (Figure 3a). These results explain why in Figure 2a high values of Π_2 lead to sandy ridges by remobilizing large volumes of sand on the shelf. On the other hand, high values of Π_2 also lead to the erosion of a larger portion of mudflat (Figure 2b, Π_3 is directly proportional to wave shear stress).

All our results fall in three categories: formation of mudflat only, formation of an erosional chenier plain, and formation of a strand plain (Figure 4a). Inner-shelf slope drives the process of mudflat or ridge creation. We can produce an alternation of these two landforms (second column in Figure 4a) or simply continue with a mudflat progression (first column of Figure 4a). Moreover, if we erode the mudflat during each storm, we generate a strand plain composed of consecutive sandy ridges without mud deposits in between (third column in Figure 4a).

Storm energy and frequency are also important for chenier formation. If mud deposition does not have enough time to form an expansive mudflat, a storm can erode all the mud leaving only a sequence of sandy ridges (strandplain, third column of Figure 4a). We also explored the effect of storm frequency and sediment concentration on mudflat extension and preservation (Figure S1). The longer is the period between two extreme storms the wider is the mudflat depositing in front of the ridge. Periods without large storms lasting 100 years build a mudflat that is 4-6 times longer than a mudflat built in 10 years. Therefore, if extreme storms are less frequent, there is a higher chance to preserve the mudflat between ridges and form an erosional chenier plain rather than a strandplain. Here, for sake of simplicity, we fix in each simulation a storm event frequency equal to one extreme event per 10 years. The remaining time is dedicated to build a mudflat under different conditions of sediment supply (Figure 2b). Future research will explore how the statistical distribution of storms and their inter-arrival times control the formation of chenier plains. Although our model results explored a fixed storm interval, additional modeling studies might be able to look at chenier plains formation as a time recorder of past storms activity.

For a given choice of parameters, Figure 4b shows through a flow chart all the possible morphological outcomes as a function of storms and deposition events. Storms with high energy are critical for the formation of sand ridges, bringing sediment to the shore (Fig. 2a). If such storms are not present, only a mudflat can form when the shelf slope is mild and cohesive sediments available. The lower is the cross-shore slope, the more likely is the formation of a mudflat (Fig. 2c). A low slope also favors the formation of a sand ridge, because waves can mobilize more sediment and move this material to the shore. Intermediate slopes prevent the formation and preservation of a mudflat, so that only a strandplain can form during storms. Finally, for high bottom slopes, neither a mudflat nor a sand ridge form, and shore progradation is absent (Table 1).

	Low wave-energy during storms	High wave-energy during storms
Low cross-shore slope	Mudflat	Chenier-plain
Intermediate cross-shore slope	No progradation	Strandplain
High cross-shore slope	No progradation	No progradation

Table 1 Formation of mudflats, chenier plains, and strandplains as a function of cross-shore slope and wave energy during storms.

Strandplains are typical of wave-dominated coasts where muddy sediments are resuspended and moved offshore by waves. Offshore of muddy coasts with large sediment supply there is a clear subaqueous slope-break, called roll-over point (Friedrichs and Wright, 2004; Eidam et al., 2017), which is controlled by sediment inputs, sediment characteristics and waves. Here we model the inner part of the shelf, onshore of the roll-over point. We therefore assume that the roll-over point is offshore of our studied area restricting the simulations to the top set of the subaqueous delta (Walsh and Nittrouer, 2009).

5. Conclusions

A non-dimensional analysis applied to a set of numerical simulations carried out with the numerical models Delft3D and SWAN sheds light on the genesis of erosional chenier plains. These landforms are characterized by the alternate deposition of two distinct units: sand ridges and mudflats. Sandy deposits are shaped by the action of waves but are mainly controlled by the inner-shelf slope. The amount of sand available at the shelf bottom plays a less important role, although at very low sand concentrations the ridge cannot form. Mudflat formation is dictated by sediment transport, accumulation, and erosion by waves, which depend on the following sediment parameters: settling velocity, sediment concentration in the water column, as well as critical shear stress for erosion. Gentle shelf slopes facilitate mudflat formation because high deposition rates overcome mild erosion by waves. The repetition of ridge and mudflat formation leads to the development of chenier plains (Figures 1b and 4a). However, depending on nearshore slope, a chenier plain may morph into a sequence of sandy beach ridges (strandplain) or a continuous mudflat losing the alternation between sand and mud. Our results provide a physically-based interpretation of the processes driving the formation of a chenier plain and partly explain why they are relatively uncommon along the shoreline (Table 1).

In order for an erosional chenier plain to form, cohesive sediments must be available in large volumes with enough sand or shell gravel that can be deposited during extreme events on the existing mudflat. During intense storms the mudflat can be eroded thus preventing the formation of a chenier system and favoring the establishment of a strandplain. Our results show that chenier genesis is less common because it depends on a specific balance between sediment availability and wave action.

Acknowledgements

This research was supported by ONR award N00014-14-1-0114 and by the National Science Foundation LTER under grants NSF 1237733 and NSF 1637630. Data are available in the following repositories: https://www.vcrlter.virginia.edu/home2/?page_id=105. We thank the Editor, two anonymous Reviewers, Dr. Travis Swanson and Dr. E. Anthony for their constructive and insightful comments.

6. References

Anthony, E.J., 1989. Chenier plain development in northern Sierra Leone, West Africa. Mar. Geol. 90, 297–309.

Anthony, E.J. (1995) Beach-ridge development and sediment supply: examples from West Africa. Mar. Geol., 129, 175–186.

Anthony, E.J., Gardel, A., Gratiot, N., Proisy, C., Allison, M.A., Dolique, F., Fromard, F., 2010. The Amazon-influenced muddy coast of South America: A review of mud bank-shoreline interactions. Earth-Science Reviews, 103, 99-129.

Anthony, E.J., Gardel, A., Gratiot, N., 2014. Fluvial sediment supply, mud banks, cheniers and the morphodynamics of the coast of South America between the Amazon and Orinoco river mouths. Geological Society, London, Special Publications, 388, 533-560.

Augustinus, P.G.E.F., 1989. Cheniers and Chenier plains: a general introduction. Mar. Geol. 90, 219–229.

Battjes, J.A., Janssen, J.P.F.M. (1978), Energy loss and set-up due to breaking of random waves, Proc. 16th Int. Conf. Coastal Eng., ASCE,569–588.

Bhattacharya, J.P., and Giosan, L., 2003, Wave-influenced deltas: geomorphological implications for facies reconstruction. Sedimentology, v. 50, p.187-210.

Berlamont, j., Ockenden, m., Toorman, e., and Winterwerp, j., 1993, The characterization of cohesive sediment properties: Coastal Engineering, v. 21, p. 105–128.

Booij, N., R. C. Ris, and L. H. Holthuijsen (1999), A third-generation wave model for coastal regions. Model description and validation, J. Geophys. Res., 104(C4), 7649–7666.

Borrego, J., Morales, J.A., Gil, N., 2000. Evolución sedimentaria reciente de la desembocadurade la Ría de Huelva (Suroeste de España). Rev. Soc. Geol. Esp. 13, 405–416.

Byrne, J.V., LeRoy, D.O., Riley, C.M., 1959. The Chenier plain and its stratigraphy, southwestern Louisiana. Trans. Gulf Coast Assoc. Geol. Soc. 9, 237–260.

Chappell, J. and Grindrod, J., 1984. Chenier plain formation in northern Australia. In: B.G. Thorn (Editor), Coastal Geomorphology in Australia. Academic Press, Sydney, pp. 197-231.

Draut, A. E., Kineke, G. C., Huh, O. K., Grymes, J. M., Westphal, K. A., Moeller, C. C., 2005. Coastal mudflat accretion under energetic conditions, Louisiana chenier-plain coast, USA. Marine Geology, 214 (2005) 27–47, doi:10.1016/j.margeo.2004.10.033.

Eidam, E., Nittrouer, C.A., Ogston, A.S., DeMaster, D.J., Liu, J.P., Nguyen, T.T., Nguyen, T.N., 2017. Dynamic controls on shallow clinoform geometry: Mekong Delta, Vietnam. Cont. Shelf Res. 147, 165–181.

Franceschini, G. and Compton, J.S. (2006) Holocene evolution of the Sixteen Mile Beach Complex, Western Cape, South Africa. J. Coastal Res., 22, 1158–1166.

Friedrichs, C.T., Wright, L.D., 2004. Gravity-driven sediment transport on the continental shelf: implications for equilibrium profiles near river mouths. Coastal Engineering 51, 795–811.

Goodfriend, G.A. and Stanley, D.J. (1999) Rapid strand-plain accretion in the northeastern Nile Delta in the 9th century AD and the demise of the port of Pelusium. Geology, 27,147–150.

Grant, W.D., O.S. Madsen (1979) Combined wave and current interaction with a rough bottom. Journal of Geophysical Research, 84(C4):1979-1808.

Harvey, N. (2006) Holocene coastal evolution: Barriers, beach ridges, and tidal flats of South Australia. J. Coastal Res., 22, 90–99.

Hasselmann, K., et al. (1973), Measurements of wind-wave growth and swell decay during the Joint North Sea Wave Project (JONSWAP), Dtsch. Hydrogr. Z. Suppl., 12(A8), 1–95, 1973.

Hein, C.J., FitzGerald, D.M., Cleary, W.J., Albernaz, M.B., de Menezes, J.T., Klein, A.H.F., 2013, Evidence for a transgressive barrier within a regressive strandplain system: Implications for complex coastal response to environmental change, Sedimentology, v. 60, p. 469-502.

Komen, G., S. Hasselmann, and K. Hasselmann (1984). On the existence of a fully developed wind-sea spectrum, J. Phys. Oceanogr. 14, 1271.

Kruit, C., 1955. Sediments of the Rhone delta, I. Grain size and microfauna. K. Ned. Geol. Mijnbouwk. Genoot. Verh., 15(3): 357-514.

Langhaar, H. (1951), Dimensional Analysis and Theory of Models, Wiley, New York.

Leonardi, N., Sun, T. and Fagherazzi, S., 2014. Modeling tidal bedding in distributary-mouth bars. Journal of Sedimentary Research, 84(6), pp.499-512.

Lesser, G., J. Roelvink, J. Van Kester, and G. Stelling (2004), Development and validation of a three-dimensional morphological model, Coastal Eng., 51, 883–915.

Morales J.A., J. Borrego, R.A. Davis, A new mechanism for chenier development and a facies model of the Saltés Island chenier plain (SW Spain), Geomorphology, 204 (2014), pp. 265–276.

Nardin, W., and S. Fagherazzi (2012). The effect of wind waves on the development of river mouth bars, Geophys. Res. Lett., 39, L12607, doi: 10.1029/2012GL051788.

Nardin, W., G. Mariotti, D. A. Edmonds, R. Guercio, and S. Fagherazzi (2013), Growth of river mouth bars in sheltered bays in the presence of frontal waves, J. Geophys. Res. Earth Surf., 118, 872–886, doi:10.1002/jgrf.20057.

Nardin, W., Curtis E. Woodcock, Sergio Fagherazzi (2016b) Bottom sediments affect Sonneratia mangrove forests in the prograding Mekong delta, Vietnam. Estuarine, Coastal and Shelf Science. 177, 60–70. Doi:10.1016/j.ecss.2016.04.019.

Nott, J., Smithers, S., Walsh, K. and Rhodes, E. (2009) Sandbeach ridges record 6000 year history of extreme tropical cyclone activity in northeastern Australia. Quatern. Sci.Rev., 28, 1511–1520.

Otvos, E.G., Price,W.A., 1979. Problems of Chenier genesis and terminology: an overview. Mar. Geol. 31, 251–263.

Park, Y., Chang, J., Lee, C., Han, S., 1996. Controls of storms and typhoons on Chenier formation in Komso Bay, western Korea. J. Coast. Res. 12, 817–822.

Partheniades, E., 1965. Erosion and deposition of cohesive soils: American Society of Civil Engineers, Journal of the Hydraulics Division, Proceedings, v. 92, p. 79–81.

Rodi, W. (1984), Turbulence models and their application in hydraulics, State-of-the-art paper article sur l'etat de connaissance." IAHR Paper presented by the IAHR-Section on Fundamentals of Division II: Experimental and Mathematical Fluid Dynamics, The Netherlands.

Roy, P.S., Cowell, P.J., Ferland, M.A. and Thom, B.G. (1994). Wave-dominated coasts. In: Coastal Evolution, Late Quaternary Shoreline Morphodynamics (Eds R.W.G. Carter and C.D. Woodroffe), pp. 121–186. Cambridge University Press, Cambridge.

Russell, E.J., Howe, H.V., 1935. Cheniers of southwestern Louisiana. Geogr. Rev. 25, 449–461.

Saito, Y.,Wei, H., Zhou, Y., Nishimura, A., Sato, Y., Yokota, S., 2000. Delta progradation and Chenier formation in the Huanghe (Yellow River) delta, China. J. Asian Earth Sci. 18,489–497.

Soulsby, R. L., A. G. Davies, J. Fredsoe, D. A. Huntley, I. G. Jonnson, D. Myrhaug, R. R. Simons, A. Temperville and T. J. Zitman, (1993a). “Bed shear stresses due to combined waves and currents.” In Abstracts-in-depth of the Marine Science and Technology G8-M overall workshop, Grenoble. 246

Tamura T., Yoshiki Saito, V. Lap Nguyen, T.K. Oanh Ta, Mark D. Bateman, Dan Matsumoto and Shota Yamashita, Origin and evolution of interdistributary delta plains; insights from Mekong River delta, Geology 2012;40;303-306, doi: 10.1130/G32717.1

van Rijn, L.C. 1993. Principles of Sediment Transport in Rivers, Estuaries, and Coastal Seas, edited, Aqua publications, Amsterdam.

Walsh, J.P. and Nittrouer, C.A., 2009. Understanding fine-grained river-sediment dispersal on continental margins. Marine Geology, 263(1-4), pp.34-45.

Woodroffe, C.D., Curtis, R., McLean, R., 1983. Development of a Chenier plain, Firth of Thames, New Zealand. Marine Geology 53, 1–22.

Woodroffe, C.D., Grime, D., 1999. Storm impact and evolution of mangrove-fringed Chenier plain Shoal Bay, Darwin, Australia. Mar. Geol. 159, 303–321.

Figure captions

Figure 1. a) Computational domain and boundary conditions. Colors show bed levels in the domain and red arrows the wave direction. Central black dashed line shows the position of the control transect for the longitudinal profile sketch. b) Example of a cross-shore section of Chenier Plain formed from an initial mudflat with sand content of 25%. Colors show sand fraction in the deposited sediments (red is sand while blue is mud). Black lines indicate different profiles of the Chenier plain during evolution. c) Aerial photographs of Louisiana coastline nearby Atchafalaya river delta, LA, USA. Image Landsat, courtesy of Google Earth, Image 2013 Terra-Metrics.

Figure 2. (a) Relationship between the dimensionless significant waves height, $\frac{\tau_{ws}}{(\rho_s-\rho_w)gD_{50}} = \frac{H_s}{D_{50}}$ imposed at the East boundary and the inner-shelf slope, *S* with the red line and crosses. Black line shows dimensionless mudflat erosion as a function of inner-shelf slope. (b) Dimensionless mudflat deposition as a function of shelf slope (with $M_e = 10^{-5}$). Black lines separate the area where a mudflat forms from the area where only a sandy ridge is present. Black and red lines in (a) and (b) plots show a transition between two geomorphic configurations as a function of basin slope, *S.* Circles with letters represent values of different coastal formation from study cases available in literature (see supplemental material).

Figure 3. Evolution of the **c**ross-shore bottom profile for two different initial slopes (solid lines). Each initial slope is subjected to two different wave climates. Dashed lines represents the final bottom profile with H_S=1m, while dashed and dotted lines are relative to H_S=3m. b) Maximum bed shear stress along *x* offshore direction at the *y* centerline. Bed sediment in the runs is composed by 90% of cohesive material with w_s=0.1 mm/s and τ_{cr}=1 Pa and 10% of non-cohesive sediment with D_{50}= 100µm.

Figure 4. a) Snapshots from 3 model runs showing longitudinal evolution, along the control transect in Figure 1a, of a prograding shoreline with different initial slopes under different wave climates and

sediment supplies. Red color means 100% sand, blue color means only mud. Each series consists of four instants of a mudflat evolving for 10 years. Black dotted lines show the initial cross-shore profile after a severe wave attack. First column: Mudflat case with initial slope S=0.013, c_m=0.4 kg/l, w_s=0.5 mm/s, τ_{cr}=1 Pa, D_{50}=100 μm and Hs=1m. Second column: Chenier Plain case formed by a series of two sandy ridges separated by a mudflat with initial slope S=0.013, c_m=0.4 kg/l, w_s=0.5 mm/s, τ_{cr}=1 Pa, D_{50}=100 μm and Hs=2m. Third column: strand plain case with initial slope S=0.013, c_m=0.4 kg/l, w_s=0.5 mm/s, τ_{cr}=0.5 Pa, D_{50}=200 μm and Hs=3m. b) A combined model of mudflats, strandplain and chenier plain generation.

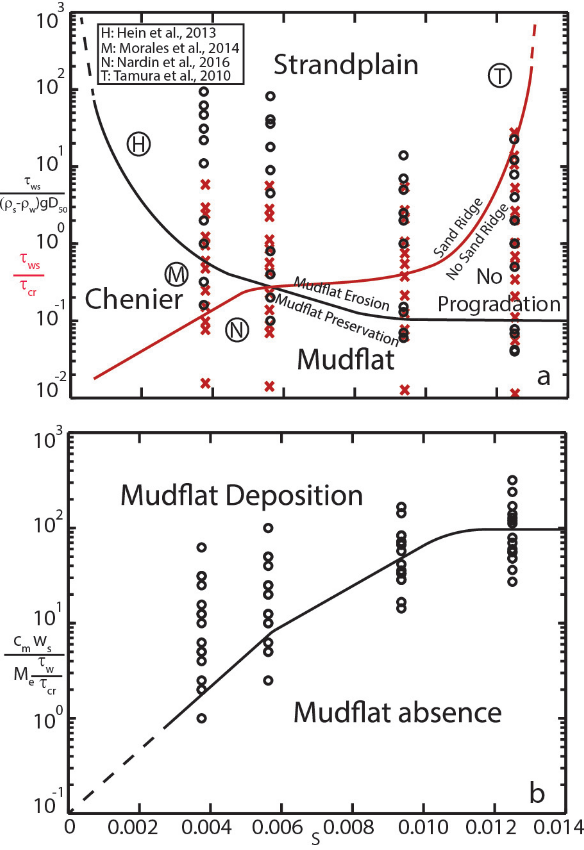

H: Hein et al., 2013
M: Morales et al., 2014
N: Nardin et al., 2016
T: Tamura et al., 2010
Strandplain
Chenier
Mudflat
No Progradation
Sand Ridge
No Sand Ridge
Mudflat Erosion
Mudflat Preservation
a
Mudflat Deposition
Mudflat absence
b
S

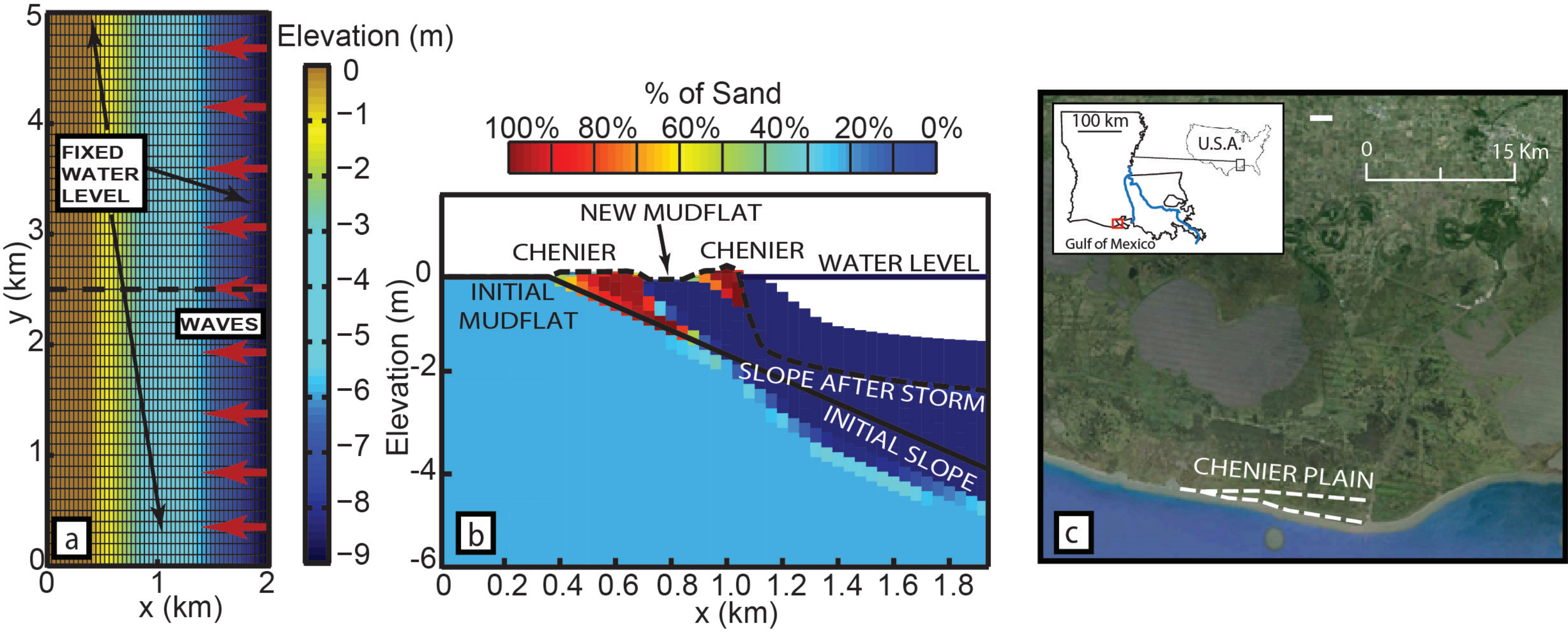

Elevation (m)
0
−1
−2
−3
−4
−5
−6
−7
−8
−9
FIXED WATER LEVEL
WAVES
y (km)
x (km)
a
% of Sand
100%
80%
60%
40%
20%
0%
NEW MUDFLAT
CHENIER
CHENIER
WATER LEVEL
INITIAL MUDFLAT
SLOPE AFTER STORM
INITIAL SLOPE
Elevation (m)
x (km)
b
100 km
U.S.A.
Gulf of Mexico
0
15 Km
CHENIER PLAIN
c

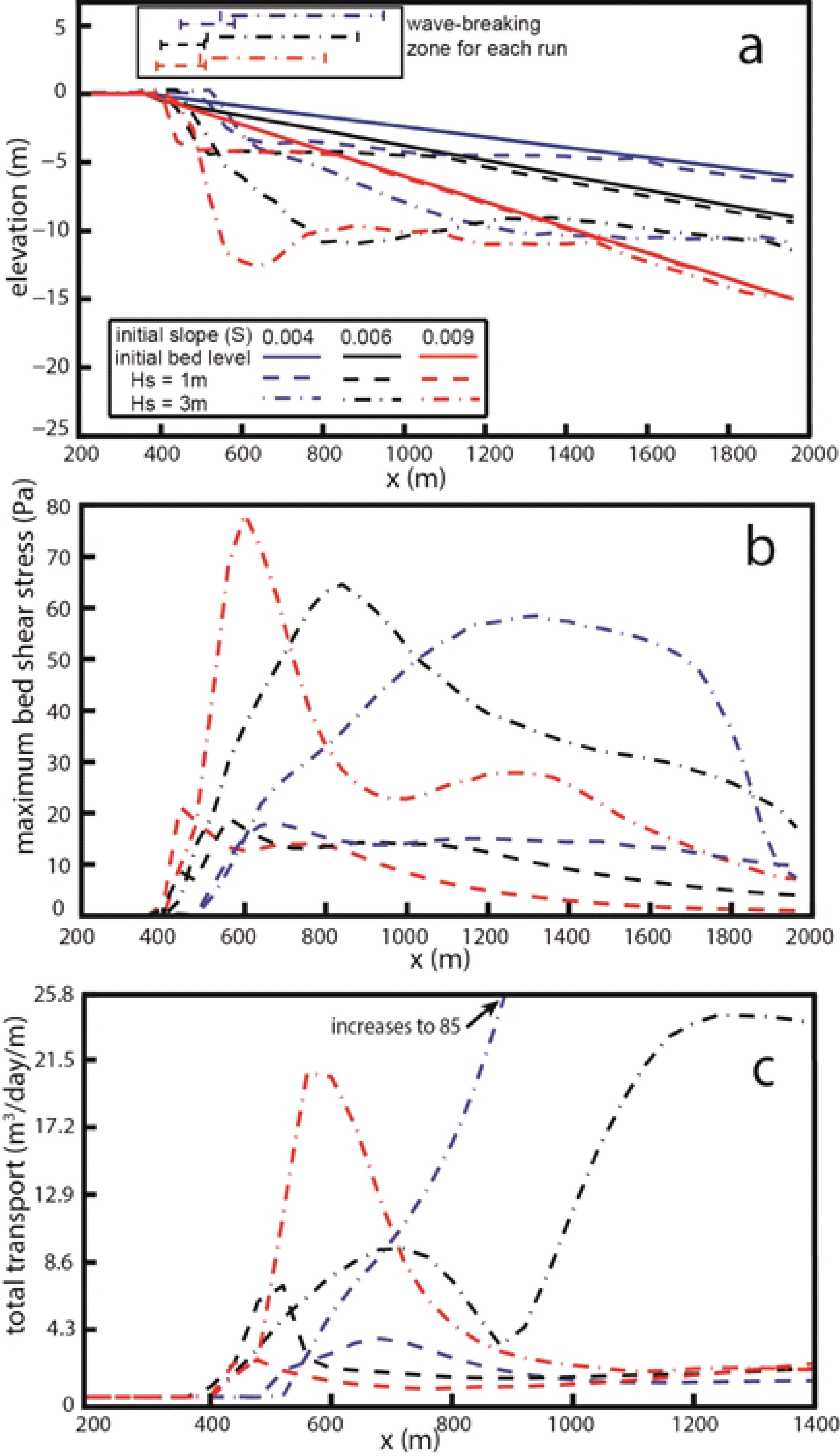

a
wave-breaking
zone for each run
elevation (m)
x (m)
initial slope (S) 0.004 0.006 0.009
initial bed level
Hs = 1m
Hs = 3m
b
maximum bed shear stress (Pa)
x (m)
c
total transport (m^3/day/m)
increases to 85
x (m)

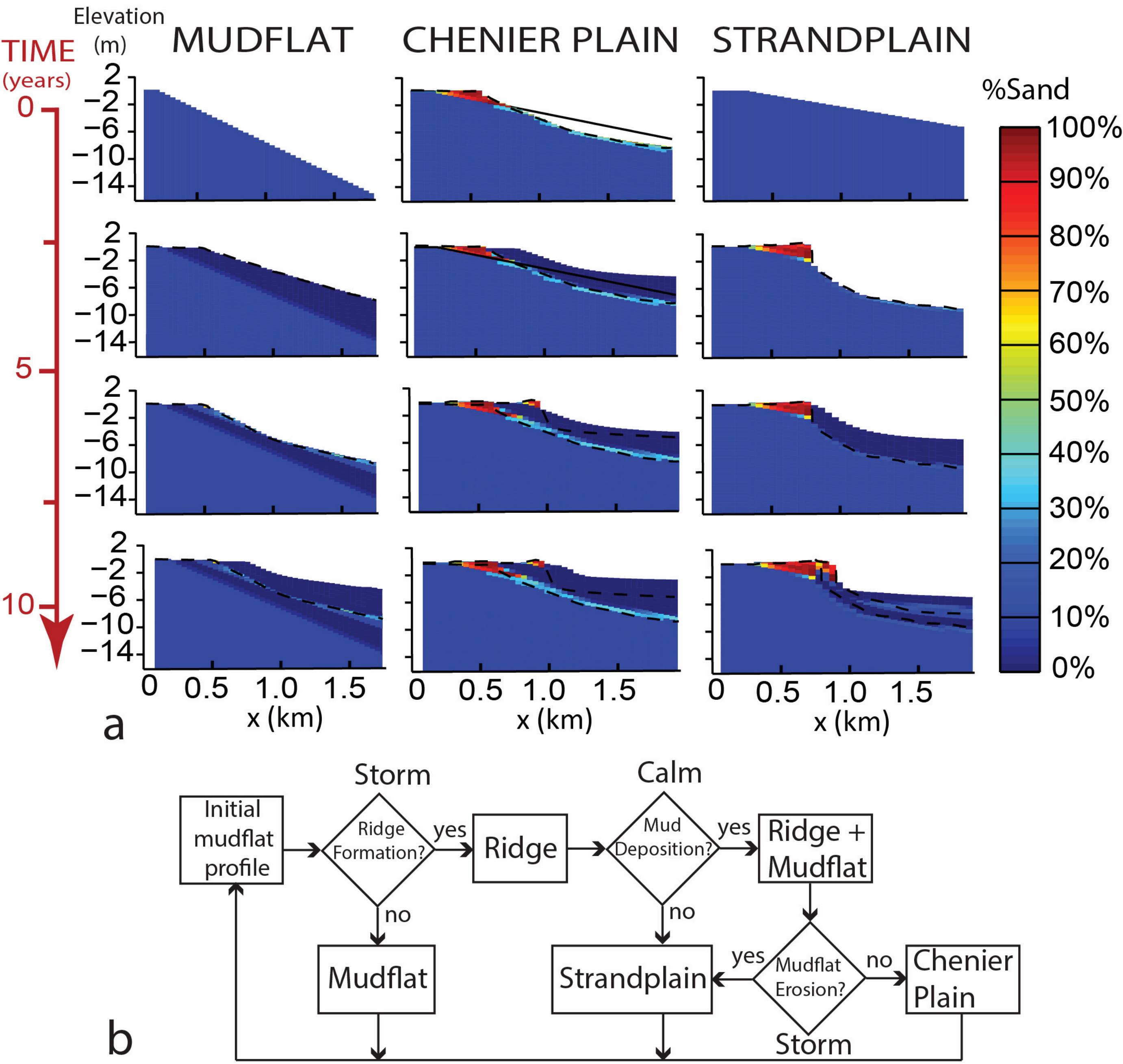

Elevation (m)
TIME (years)
MUDFLAT
CHENIER PLAIN
STRANDPLAIN
%Sand
100%
90%
80%
70%
60%
50%
40%
30%
20%
10%
0%
0
5
10
2
−2
−6
−10
−14
0
0.5
1.0
1.5
x (km)
a
Storm
Calm
Initial mudflat profile
Ridge Formation?
yes
no
Ridge
Mud Deposition?
yes
no
Ridge + Mudflat
Mudflat
Strandplain
Mudflat Erosion?
yes
no
Chenier Plain
Storm
b